# Sterol Structure and Sphingomyelin Acyl Chain Length Modulate Lateral Packing Elasticity and Detergent Solubility in Model Membranes

Xin-Min Li, Maureen M. Momsen, Howard L. Brockman, and Rhoderick E. Brown
The Hormel Institute, University of Minnesota, Austin, Minnesota

ABSTRACT Membrane microdomains, such as caveolae and rafts, are enriched in cholesterol and sphingomyelin, display liquid-ordered phase properties, and putatively function as protein organizing platforms. The goal of this investigation was to identify sterol and sphingomyelin structural features that modulate surface compression and solubilization by detergent because liquid-ordered phase displays low lateral elasticity and resists solubilization by Triton X-100. Compared to cholesterol, sterol structural changes involved either altering the polar headgroup (e.g., 6-ketocholestanol) or eliminating the isooctyl hydrocarbon tail (e.g., 5-androsten-3$\beta$-ol). Synthetic changes to sphingomyelin resulted in homogeneous acyl chains of differing length but of biological relevance. Using a Langmuir surface balance, surface compressional moduli ($C_s^{-1}$) were assessed at various surface pressures including those ($\pi \geq 30$ mN/m) that mimic biomembrane conditions. Sphingomyelin-sterol mixtures generally were less elastic in a lateral sense than chain-matched phosphatidylcholine-sterol mixtures at equivalent high sterol mole fractions. Increasing content of 6-ketocholestanol or 5-androsten-3$\beta$-ol in sphingomyelin decreased lateral elasticity but much less effectively than cholesterol. Our results indicate that cholesterol is ideally structured for maximally reducing the lateral elasticity of membrane sphingolipids, for enabling resistance to Triton X-100 solubilization, and for interacting with sphingomyelins that contain saturated acyl chains similar in length to their sphingoid bases.

## INTRODUCTION

Sterols are omnipresent lipids in eukaryotes and carry out indispensable roles in regulating the physical properties of biomembranes (Simons and Ikonen, 2000; Ohvo-Rekilä et al., 2002). The enrichment of different sterols in select membranes suggests specialized functionality. One putative structural role for cholesterol is as a key and integral component of membrane microdomains such as caveolae and rafts. These microdomains, which are enriched in sphingolipids as well as cholesterol, have been proposed to function as organizing platforms for proteins with certain kinds of lipid anchors, including key signaling proteins (Brown and Rose, 1992; Simons and Ikonen, 1997; Brown and London, 2000). It has been suggested that the tight packing within liquid-ordered (LO) sphingolipid-cholesterol mixtures is a key physical property that enables rafts to resist solubilization by Triton X-100 and modulates the lateral localization of certain lipid-anchored proteins (Schroeder et al., 1994, 1998; Smaby et al., 1996a,b; Ahmed et al., 1997; Brown, 1998). LO phase is liquidlike with respect to lipid lateral diffusion, but ordered in that lipid acyl chains have reduced *gauche* rotomers and are extended because of interactions with the planar rings of cholesterol (Ipsen et al., 1987). Cholesterol mole fractions exceeding 0.25 are necessary to form LO phase in phosphatidylcholine (PC) mixtures depending upon acyl chain structural features. Low cholesterol content results in liquid-disordered phase behavior (Edidin, 2003; Silvius, 2003).

In lipid model membranes containing either sphingomyelin (SM) or saturated PCs, increasing the cholesterol content above 0.25 mole fraction results in high lipid packing densities characterized by dramatically decreased lateral elasticity (Evans and Needham, 1987; Needham and Nunn, 1990; McIntosh et al., 1992; Smaby et al., 1994, 1996a, 1997; Li et al., 2001). In general, the low lateral elasticity that is characteristic of SM-cholesterol and saturated PC-cholesterol mixtures correlates with elevated resistance to solubilization by Triton X-100 (Li et al., 2001), an empirical feature of raft lipid mixtures (London and Brown, 2000; Sot et al., 2002; Luria et al., 2002). Among saturated chain PCs, dipalmitoyl PC (DPPC) has been an especially popular raft lipid because its saturated acyl chains and phosphorylcholine headgroup duplicate certain of the important structural features of SM, and DPPC forms LO phase upon mixing with adequate amounts of cholesterol (Sankaram and Thompson, 1990; Schroeder et al., 1998; Xu and London, 2000). Even so, the lateral elasticity is lower in SM-cholesterol mixtures compared to their chain-matched PC-cholesterol mixtures (Li et al., 2001). This finding points out differences in the physical environments of SM-cholesterol and saturated PC-cholesterol mixtures and suggests that saturated PCs might not display all of the key features that predispose SMs to form microdomains.

*Submitted May 2, 2003, and accepted for publication August 8, 2003.*

Address reprint requests to Dr. Rhoderick E. Brown, The Hormel Institute, University of Minnesota, 801 16th Avenue NE, Austin, MN 55912-3698. Tel.: 507-433-8804; Fax: 507-437-9606; E-mail: reb@tc.umn.edu or rebrown@hi.umn.edu.

Xin-Min Li's present address is Molecular Medicine, M/C NRC-3, Oregon Health & Science University, Portland, OR 97239.

*Abbreviations used*: LO, liquid-ordered; SM, sphingomyelin; PC, diacyl-*sn*-glycero-3-phosphocholine; di-16:0 PC or DPPC, dipalmitoyl-*sn*-glycero-3-phosphocholine; 16:0 SM, *N*-palmitoyl sphingosylphosphocholine; 18:0 SM, *N*-stearoyl sphingosylphosphocholine; 14:0–16:0 PC or MPPC, 1-myristoyl-2-palmitoyl-*sn*-glycero-3-phosphocholine; 14:0–18:0 PC or MSPC, 1-myristoyl-2-stearoyl-*sn*-glycero-3-phosphocholine; 24:0 SM, *N*-lignoceroyl sphingosylphosphocholine; 26:0 SM, *N*-26:0 sphingosylphosphocholine.



0006-3495/03/12/3788/14 $2.00

It has recently been suggested that certain sterol derivatives act in anticholesterol fashion in that they abolish or weaken rafts by interfering with LO phase formation (Xu and London, 2000; Xu et al., 2001). Here, we have directly assessed the capacity of two different sterols to produce packing states displaying low lateral elasticity, a characteristic of the cholesterol-induced LO phase. We investigated sterols containing either modified polar headgroup moieties (e.g., 6-ketocholestanol) or missing the isooctyl hydrocarbon chain (e.g., 5-androsten-3$\beta$-ol) and their mixing interactions with SMs containing different homogeneous acyl chains commonly found in nature (Fig. 1). We employed Langmuir film balance approaches to study the interfacial interactions of the lipid mixtures. This experimental system permits lipid mixing behavior and lateral interactions to be investigated over the range of molecular areas known to occur in biomembranes while avoiding changes in the overall mesomorphic organization that often occur in bulk-hydrated dispersions (e.g., bilayer vesicles) as lipid composition is varied. Lipid monolayers and bilayers share most of the relevant physical properties known to occur in membranes (e.g., Möhwald, 1995), including the LO phase, which was first defined and modeled in two-dimensional monolayer lattices of cholesterol and DPPC (Ipsen et al., 1987). We find that changes to sterol structure, such as those found in androsterol and 6-ketocholestanol, strongly diminish their capacity to mimic cholesterol. Understanding the physical properties of various sterol derivatives extends beyond the raft microdomain field because sterols such as 6-ketocholestanol have been used as tools to control uncoupler effects on mitochondrial membrane potential (Chávez et al., 1996; Starkov et al., 1994, 1997) as well as to modulate hydrophobic ion binding and transport (Franklin and Cafiso, 1993), peptide binding and insertion (Cladera and Oshea, 1998; Voglino et al., 1998), and monovalent cation conductance in bilayers (Rokitskaya et al., 1997, 2002).

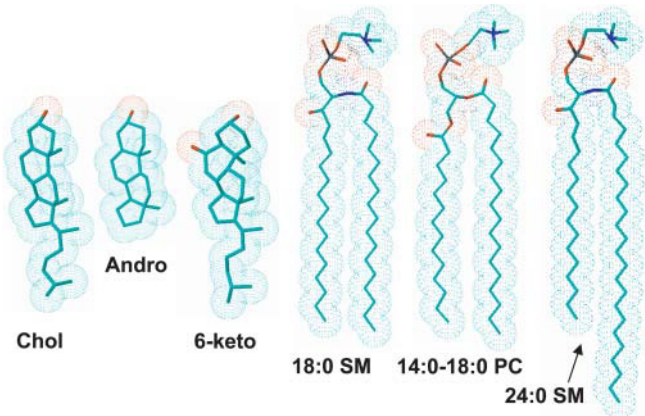


FIGURE 1 Structural features of cholesterol, androsterol, 6-ketocholestanol, sphingomyelin (*SM*), and phosphatidylcholine (*PC*). Blue centers represent nitrogen atoms and red centers represent oxygen atoms. For simplicity, lipid hydrocarbon chains are depicted as fully extended trans rotamers. In reality, free rotation about the carbon-carbon single bonds produces *trans-gauche* isomers which are more numerous in the fluid state than in the gel state. Chain-matching of PC and SM is best achieved when PC contains a myristoyl *sn*-1 chain, as illustrated for 18:0 SM and 14:0–18:0 PC. Long saturated acyl chains (e.g., 24:0) produce chain length asymmetry within the SM molecule (*arrow*).

## MATERIALS AND METHODS

### Chemicals

5-androsten-3$\beta$-ol (androsterol) and 6-ketocholestanol were purchased from Steraloid (Wilton, NH). All PCs were obtained from Avanti Polar Lipids (Alabaster, AL). SMs containing homogeneous acyl chains were synthesized by reacylating sphingosylphosphorylcholine with the *N*-hydroxysuccinimide ester of the desired fatty acid (Li et al., 2000, 2001). After purification by flash column chromatography and crystallization from $CHCl_3/CH_3OH$ using –20°C acetone, all lipids were >99% pure by TLC analysis. Acyl homogeneity of the SM derivatives was confirmed by quantitatively releasing, methylating, and analyzing the fatty acyl residues via capillary gas chromatography (Smaby et al., 1996a,b). SMs and PCs were quantitated by phosphate assay (Bartlett, 1959) whereas sterols were quantitated gravimetrically.

Fig. 1 shows the structures of representative SM and PC species used in the present study. Chain-matching of PC to SM, with respect to hydrocarbon conformation and length, requires PC to have a myristoyl *sn*-1 chain and an *sn*-2 chain identical with that of SM (Brown, 1998; Li et al., 2001, and references within). This situation arises because the first three carbons of the 18-carbon sphingoid base in SM are similar, but not identical, to the glycerol backbone configuration of PC. By virtue of being ester-linked, saturated *sn*-1 acyl chains of 14 carbons in PC closely match the 18-carbon sphingoid base of SM with respect to hydrocarbon length. In SM, the second carbon of sphingosine, the amide linkage consisting of the 2-amino group of sphingosine and the carbonyl group of the acyl chain, along with the first two carbons of the N-linked acyl chain, form a co-planar segment that projects roughly orthogonal to the long axis of the sphingosine hydrocarbon chain and parallel to the bilayer interface. However, between carbons 2 and 3, the acyl chain bends sharply to become parallel to the sphingoid base chain. One consequence of this bend is axial displacement between the carbon atoms of the two hydrocarbon chains causing positional inequivalence. Analogous positional inequivalences exist within the *sn*-1 and *sn*-2 ester-linked acyl chains of phosphoglycerides acyl chains. Also shown in Fig. 1 are the structural features of 6-ketocholestanol (keto group in the B-ring of the cholestane ring assembly), 5-androsten-3$\beta$-ol (no isooctyl hydrocarbon tail), and cholesterol.

### Langmuir film balance conditions

Water for the subphase buffer was purified by reverse osmosis, activated charcoal adsorption, and mixed-bed deionization; then was passed through a Milli-Q UV Plus System (Millipore, Bedford, MA), and filtered through a 0.22-$\mu$m Millipak 40 Membrane. Subphase buffer (pH 6.6) consisting of 10 mM potassium phosphate, 100 mM NaCl, and 0.2% $NaN_3$ was stored under argon until use. Glassware was acid-cleaned, rinsed thoroughly with deionized water, and then with hexane/ethanol (95:5) before use. Lipid stock solutions were prepared in hexane/ethanol (95:5) or hexane/isopropanol/water (70:30:2.5). Solvent purity was verified by dipole potential measurements (Smaby and Brockman, 1991).

Surface pressure-molecular area ($\pi$-A) isotherms were measured using a computer-controlled, Langmuir-type film balance, calibrated according to the equilibrium spreading pressures of known lipid standards (Momsen et al., 1990). Lipids were mixed and spread (51.67 $\mu$l aliquots) from dissolved stock solutions. Films were compressed at a rate of $\leq$4 Å$^2$/mol/min after an

initial delay period of 4 min. The standard errors of the isotherms were routinely <2%. The subphase was maintained at fixed temperature using a thermostatic, circulating water bath. The film balance was housed in an isolated laboratory supplied with clean air by a Bioclean Air Filtration system equipped with charcoal and HEPA filters. The trough was separately enclosed under humidified argon, cleaned by passage through a seven-stage series filtration setup consisting of an Alltech activated charcoal gas purifier, a LabClean filter, and a series of Balston disposable filters consisting of two adsorption (carbon) and three filter units (93% and 99.99% efficiency at 0.1 $\mu$m). Film balance features that contribute to isotherm reproducibility include automated lipid spreading via a modified HPLC autoinjector, automated surface cleaning by multiple barrier sweeps between runs, and highly accurate, reproducible setting of the subphase level by an automated aspirator.

## Isotherm analysis

In keeping with recent proposals, we avoid using the term *liquid condensed* and instead use the term *condensed* to denote monolayer states in which the hydrocarbon chains are ordered (Kaganer et al. 1999). The liquid-expanded state differs from the condensed state in that the chains are conformationally disordered. Monolayer phase transitions between the liquid-expanded and condensed states were identified from the second and third derivatives of surface pressure ($\pi$) with respect to molecular area ($A$) as previously described (Ali et al., 1998; Li et al., 2000).

Experimental monolayer compressibilities were obtained from $\pi$-$A$ data at the indicated lipid mixing ratios using

$$C_s = (-1/A)(dA/d\pi), \quad (1)$$

where $A$ is the area per molecule at the indicated surface pressure and $\pi$ is the corresponding surface pressure. The ideal mixing behavior of the lipids was modeled by apportioning the $C_s$ value for each lipid (as a pure entity) by both molecular area fraction and mole fraction as described previously (Ali et al., 1994; Smaby et al., 1997; Li et al., 2002).Thus, at a given constant surface pressure ($\pi$),

$$C_s = (1/A)[(C_{s1}A_1)X_1 + (C_{s2}A_2)X_2], \quad (2)$$

where $X_2 = (1 - X_1)$ and $C_s$ is additive with respect to the product, $C_{si}A_i$, rather than $C_{si}$, for either ideal or completely nonideal mixing. Deviation of experimental values from calculated ideality indicate that the lipid components of the mixed monolayers are partially nonideally mixed. The data were expressed as the surface compressional moduli ($C_s^{-1}$), which Davies and Rideal (1963) originally defined as the reciprocal of isothermal compressibility, to facilitate comparisons with bulk elastic moduli of area compressibility measurements made in bilayers (e.g., Evans and Needham, 1987; Needham and Nunn, 1990). We used a 100-point sliding window that utilized every fourth point to calculate a $C_s^{-1}$ value before advancing the window one point. Reducing the window size by as much as fivefold did not significantly affect the $C_s^{-1}$ values obtained. Each $C_s^{-1}$ vs. average molecular area curve consisted of 200 $C_s^{-1}$ values obtained at equally spaced molecular areas along the $\pi$-A isotherms. High $C_s^{-1}$ values correspond to low lateral elasticity. The standard errors of the $C_s^{-1}$ values are ~2%. As previously shown (Li et al., 2001), the $C_s^{-1}$ values of PC-cholesterol and SM-cholesterol mixed monolayers are strongly affected by PC and SM acyl structure. When mixed with equivalent high cholesterol mole fractions, PCs and SMs with saturated acyl chains have much higher $C_s^{-1}$ values (lower lateral elasticity) than PCs (and SMs) with unsaturated acyl chains, suggesting that *cis* double bonds can act as interfacial ''springs'' that mitigate the capacity of cholesterol to reduce lateral elasticity (Smaby et al., 1997). Comparisons of monolayer $C_s^{-1}$ values with bilayer area compressional moduli for POPC show the expected ~twofold difference in magnitude at high monolayer surface pressures (>30 mN/m) (Smaby et al., 1996b), in agreement with other experimental approaches indicating that the high pressure region of monolayers mimics the biomembrane environment (Marsh, 1996; MacDonald, 1996). More comprehensive discussion of the micromechanical properties and two-dimensional elasticity of model membranes is provided by Needham (1995) and Behroozi (1996), respectively.

## Assessment of lipid resistance to detergent solubilization by light scattering

Lipid solubilization by Triton X-100 was determined by light scattering as described previously (Li et al., 2001). Multilamellar lipid vesicles (500 nmol lipid) were prepared in 10 mM HEPES (pH 6.6) containing 100 mM NaCl and 0.02% $NaN_3$ by briefly vortexing the hydrated lipid at temperatures 20–25°C above their thermal phase transitions and then cooling to room temperature for 4 h. As also noted by Xu and London (2000), we found the preceding approach to reduce variation associated with detergent solubilization data. Each lipid mixture was divided in half after preparation. One half served as a control (no Triton X-100), and the remaining half was mixed with Triton X-100 to achieve a 15.5:1 molar ratio (detergent:lipid), similar to ratios used previously (Ahmed et al., 1997; Xu and London, 2000). Controls and detergent-treated samples were incubated for 12 h at 24°C before measuring their optical densities at 400 nm. Solubilization of lipid resulted in decreased light scattering and was expressed ratiometrically as the percent reduction in OD by dividing the OD of the sample mixed with Triton-X 100 by the OD of the detergentless control. Incubations carried out for up to 24 h showed that changes in OD occurred during the first 3 h after Triton X-100 addition. Control measurements utilizing light scattering at 90° in a steady-state spectrofluorimeter (Mattjus et al., 1999) yielded similar results.

# RESULTS

## The effects of androsterol and 6-ketocholestanol on the two-dimensional phase behavior of SMs and chain-matched PCs

Fig. 2 shows the effect of mixing androsterol with 16:0 SM, 14:0–16:0 PC, 18:0 SM, and 14:0–18:0 PC. Included are both the surface pressure ($\pi$) versus mean molecular area (*upper panels*) and the surface compressional moduli ($C_s^{-1}$) versus mean molecular area (*lower panels*), at sterol mole fractions (0–0.6) covering the range that cholesterol is found in biological membranes. Fig. 3 shows how 6-ketocholestanol affects the interfacial behavior of the same lipids (16:0 SM and 14:0-16:0 PC, 18:0 SM, and 14:0–18:0 PC). Two-dimensional phase transitions are evident in the SM and PC isotherms in the absence of sterol (Figs. 2 and 3; *upper panel*, *far right isotherms*). Slightly higher onset surface pressures are observed for the PCs compared to the respective SMs, consistent with our earlier findings (Li et al., 2001). At a mole fraction of androsterol or 6-ketocholestanol >0.3, the two-dimensional transitions associated with the SMs and PCs became undetectable. This was clearly evident in the $C_s^{-1}$ vs. mean molecular area plots (Figs. 2 and 3; *lower panels*), which showed characteristic ''troughs'' in the two-phase coexistence region due to differences in the partial molar areas of the liquid-expanded (chain-disordered) and condensed (chain-ordered) phases. The disappearance of the liquid expanded-to-condensed transition produced by androsterol or 6-ketocholestanol is a general effect that is also observed upon mixing with cholesterol.

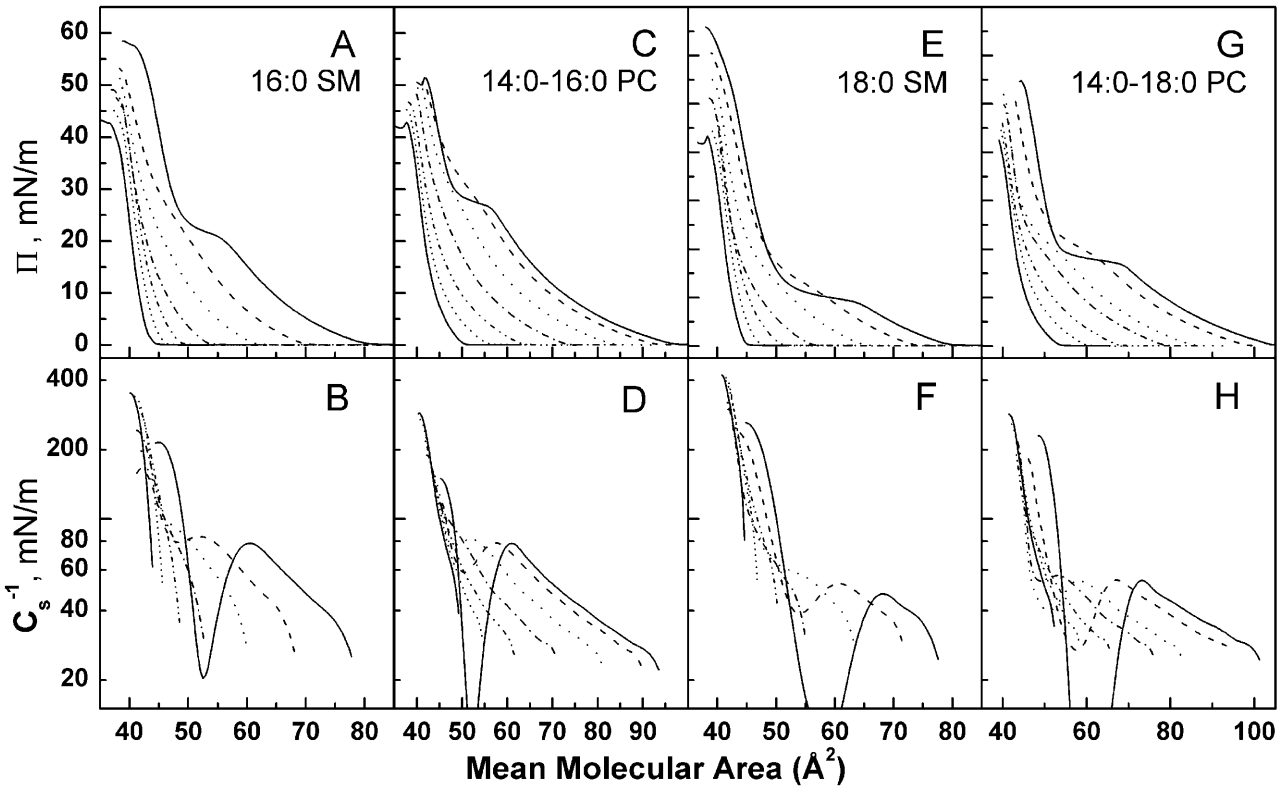


FIGURE 2 Monolayer behavior of androsterol mixed with 16:0 SM, 14:0–16:0 PC, 18:0 SM, or 14:0–18:0 PC. Data were collected using the automated Langmuir-type film balance described in text. (*Upper panels*) Surface pressure vs. average molecular area isotherms. (*Lower panels*) Surface compressional modulus ($C_s^{-1}$) vs. average molecular area. Mole fraction of sterol (*from right to left*), 0 (———), 0.1 (- - -), 0.2 (· · · ·), 0.3 (— · —), 0.4 (— · · —), 0.5 (. . . .), and 0.6 (——). Isotherms of cholesterol mixed with these same species of SM and PC have been reported previously (Li et al., 2001, Figs. 2 and 3).

### Androsterol and 6-ketocholestanol reduce the lateral elasticity of SM more than that of chain-matched PC

Figs. 4 and 5 illustrate how increasing mole fraction of androsterol and 6-ketocholestanol affect the lateral elasticity of 16:0 SM, 14:0–16:0 PC, 18:0 SM, and 14:0–18:0 PC at various constant surface pressures. Noteworthy are the effects of each sterol at higher surface pressures (e.g., 30 mN/m) that simulate biomembrane conditions with respect to lipid cross-sectional areas (MacDonald, 1996; Marsh, 1996). Upon mixing either sterol at low mole fraction with the SMs or PCs (Fig. 4 and 5, ♦), clearcut decreases were observed in the $C_s^{-1}$ values until sterol content reached ~10–15 mol %. The response was observed only at 30 mN/m (♦) and not at 5 (●) or 15 mN/m (▲). The initial drops in $C_s^{-1}$ values indicated an increase in lateral elasticity, consistent with low sterol content disrupting and disordering the gel phase. Further elevation of sterol content caused steady increases in the $C_s^{-1}$ values.

At high sterol mole fraction, the $C_s^{-1}$ values of SM were affected to a greater degree than those of PC. Including 40 mol % of either androsterol or 6-ketocholestanol with 18:0 SM increased the $C_s^{-1}$ values ~1.7-fold compared to its pure condensed state, i.e., gel phase (Figs. 4 *C* and 5 *C*). With 16:0 SM, the sterol-induced increases in $C_s^{-1}$ values were ~1.75-fold for androsterol and ~1.9-fold for 6-ketocholestanol at 0.4 mole fraction of sterol (Figs. 4 *A* and 5 *A*). With 14:0–18:0 PC, the sterol-induced increases in $C_s^{-1}$ values were ~1.1-fold for androsterol and ~1.5-fold for 6-ketocholestanol at 0.4 mole fraction of sterol (Figs. 4 *D* and 5 *D*). Because the two-dimensional phase transition of 14:0–16:0 PC occurred close to 30 mN/m, the low $C_s^{-1}$ value of pure 14:0–16:0 PC reflected mixed phase rather than homogeneous condensed phase, i.e., gel, and complicated direct comparison with the 18:0 SM, 16:0 SM, and 14:0–18:0 PC data.

In addition to the relative changes in the $C_s^{-1}$ values caused by the sterols, it also was evident that the SMs required less sterol than the PCs to achieve equivalent high $C_s^{-1}$ values, i.e., low lateral elasticity. With 16:0 SM and 14:0–16:0 PC at 30 mN/m, equivalent $C_s^{-1}$ values were produced by mixing with ~35 mol % and 55 mol % of androsterol, respectively; whereas, equivalent $C_s^{-1}$ values were produced by 6-ketocholestanol at ~35 mol % and 50 mol %. In 18:0 SM and 14:0–18:0 PC at 30 mN/m, equivalent $C_s^{-1}$ values were produced by mixing with ~35 mol % and 50 mol % of 6-ketocholestanol, although only 20

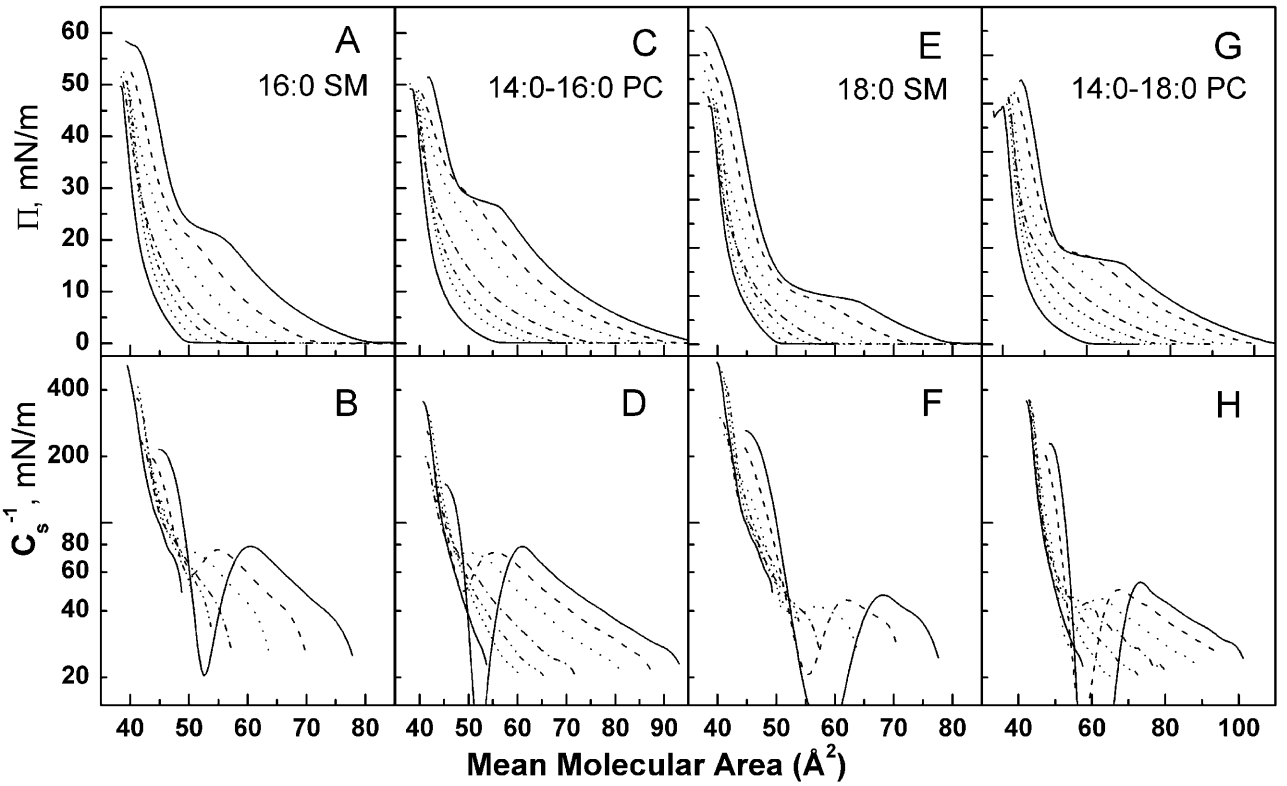


FIGURE 3 Monolayer behavior of 6-ketocholestanol mixed with 16:0 SM, 14:0–16:0 PC, 18:0 SM, or 14:0–18:0 PC. Other details are the same as in the Fig. 2 legend.

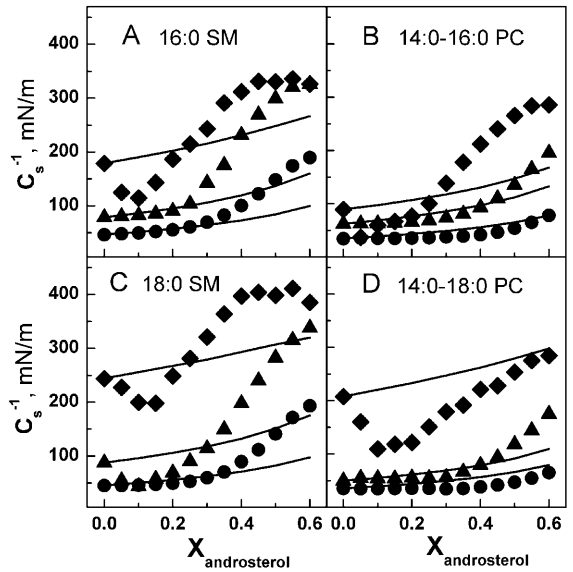


FIGURE 4 Surface compressional moduli ($C_s^{-1}$) vs. sterol mole fraction analyses. (*A*) 16:0 SM/androsterol; (*B*) 14:0–16:0 PC/androsterol; (*C*) 18:0 SM/androsterol; and (*D*) 14:0–18:0 PC/androsterol. The different symbols represent values calculated from experimental data at the following surface pressures: 5 mN/m (●), 15 mN/m (▲), and 30 mN/m (♦). Solid lines represent predicted response assuming additivity of individual lipid components (see text). Values for mixtures of cholesterol with these same species of SM and PC have been reported previously (Li et al., 2001, Fig. 6).

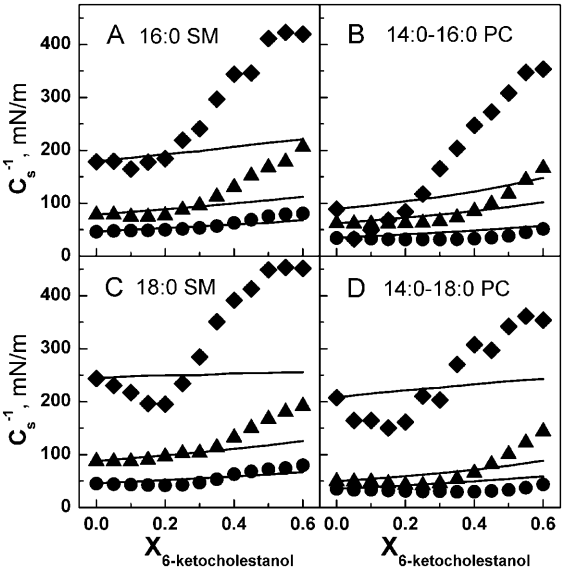


FIGURE 5 Surface compressional moduli ($C_s^{-1}$) vs. sterol mole fraction analyses. (*A*) 16:0 SM/6-ketocholestanol; (*B*) 14:0–16:0 PC/6-ketocholestanol; (*C*) 18:0 SM/6-ketocholestanol; and (*D*) 14:0–18:0 PC/6-ketocholestanol mixed monolayers. The different symbols represent values calculated from experimental data at the following surface pressures: 5 mN/m (●), 15 mN/m (▲), and 30 mN/m (♦). Solid lines represent predicted response assuming additivity of individual lipid components (see Materials and Methods).

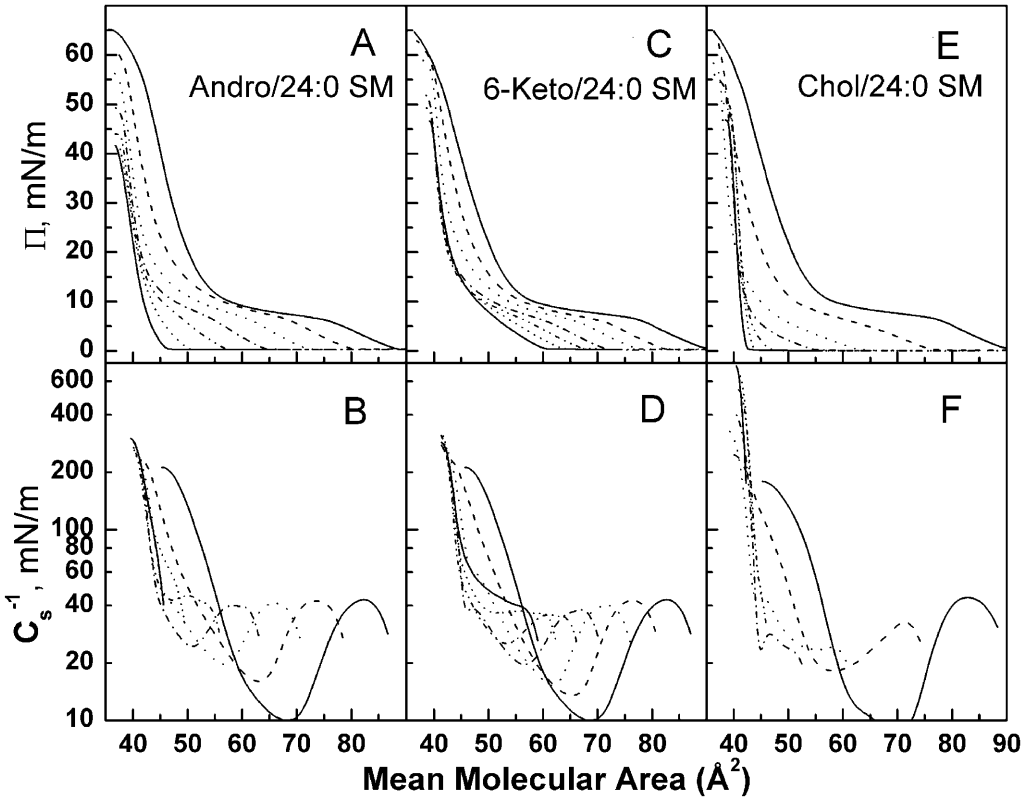


FIGURE 6 Monolayer behavior of different sterols mixed with 24:0 SM. (*Upper panels*) Surface pressure versus average molecular area isotherms. (*Lower panels*) Surface compressional modulus ($C_s^{-1}$) vs. average molecular area. (*A*, *B*) 24:0 SM/androsterol; (*C*, *D*) 24:0 SM/6-ketocholesterol; and (*E*, *F*) 24:0 SM/cholesterol mixed monolayers. Mole fraction of sterol (*from right to left*), 0 (———), 0.1 (- - -), 0.2 (· · · ·), 0.3 (— · —), 0.4 (— · · —), 0.5 (. . . .), and 0.6 (——).

mol % androsterol was needed in 18:0 SM to produce similar $C_s^{-1}$ values as 50 mol % mixed with 14:0–18:0 PC.

The 30-mN/m experimental data in Figs. 4 and 5 displayed still another noteworthy response. When androsterol mole fraction rose above 0.4–0.45, the $C_s^{-1}$ values of 16:0 SM and 18:0 SM no longer increased, but remained approximately constant. With 6-ketocholestanol, 0.5 or higher mole fraction had to be reached for the lateral elasticity to become constant. In contrast, no clearcut plateauing of the $C_s^{-1}$ values was observed when either sterol was mixed with 14:0–16:0 PC (Figs. 4 *B* and 5 *B*) and 14:0–18:0 PC (Figs. 4 *D* and 5 *D*) at 30 mN/m. At lower surface pressures (e.g., 15 mN/m), the plateauing of the $C_s^{-1}$ values at high sterol mole fraction was not observed in the SMs. The plateauing response appears likely to be related to the lateral elasticity of the pure sterols. The $C_s^{-1}$ values of pure androsterol monolayers were 361, 393, and 324 mN/m at 10, 20, and 30 mN/m, respectively, and the $C_s^{-1}$ values of pure 6-ketocholestanol monolayers were 109, 169, and 233 mN/m at 10, 20, and 30 mN/m. The values were much lower than those of pure cholesterol monolayers (e.g., $C_s^{-1}$ values of 1126, 1551, and 1540 mN/m at 10, 20, and 30 mN/m, respectively; Merkel and Sackmann, 1994; Li et al., 2002).

In Figs. 4 and 5, the solid lines represent theoretical ideal mixing calculated from the $C_s^{-1}$ values of pure sterol and pure SM (or PC) and apportioned based on both mole fraction and area fraction (Smaby et al., 1997; Li et al., 2002). Because of this apportioning, the theoretical ideal mixing lines are curvilinear with the degree of nonlinearity depending on the $C_s^{-1}$ values of the pure sterols. At low surface pressures (e.g., 5 mN/m), the lateral elasticities were relatively unaffected and followed the theoretical ideal mixing closely between 0 and 0.6 mole fraction 6-ketocholestanol in both SM and PC (Fig. 5, *A–D*, *lower solid lines*). With androsterol, similar behavior was observed only in the PC mixtures (Fig. 4, *B* and *D*). When androsterol mole fraction exceeded 0.3–0.35 in SM, significant positive deviations occurred in the $C_s^{-1}$ values compared to theoretical ideal mixing (Fig. 4, *A* and *C*). At high surface pressures (e.g., 30 mN/m), the already high $C_s^{-1}$ values characteristic of the condensed phase SM and PC immediately dipped below theoretical ideal mixing values, but then increased dramatically and showed strong positive deviations from theoretical ideal mixing as sterol mole fraction exceeded 0.25 for SM. With androsterol, the large positive deviations were present with SM but not with 14:0–18:0 PC. With 6-ketocholestanol, the positive deviations occurred in both SMs and 14:0–18:0 PC but were larger for SM than for 14:0–18:0 PC. In the case of pure 14:0–16:0 PC, $C_s^{-1}$ values at 30 mN/m were influenced (lowered) because of proximity to the two-dimensional-phase transition. The net effect was to produce a theoretical ideal curve with low $C_s^{-1}$ values (Figs. 4 *B* and 5 *B*, *solid lines*) and complicate direct comparison with the 18:0 SM, 16:0 SM, and 14:0–18:0 PC

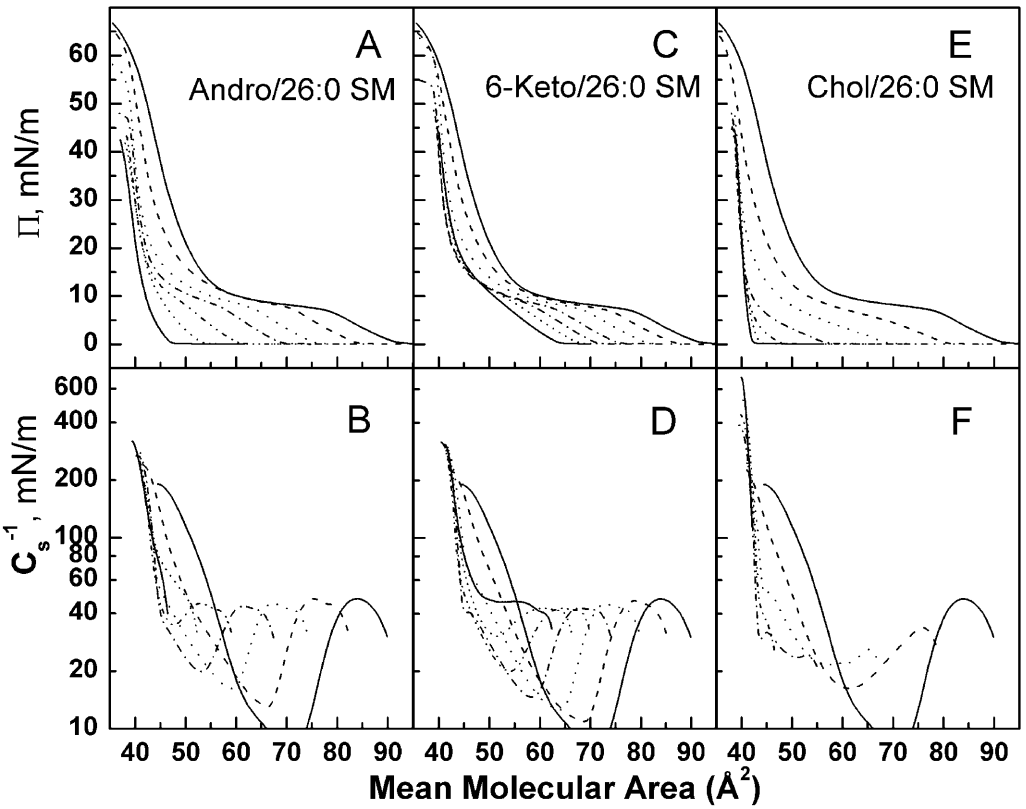


FIGURE 7 Monolayer behavior of different sterols mixed with 26:0 SM. (*Upper panels*) Surface pressure versus average molecular area isotherms. (*Lower panels*) Surface compressional modulus ($C_s^{-1}$) vs. average molecular area. (*A*, *B*) 26:0 SM/androsterol; (*C*, *D*) 26:0 SM/6-ketocholesterol; and (*E*, *F*) 26:0 SM/cholesterol mixed monolayers. Mole fraction of sterol (*from right to left*), 0 (———), 0.1 (- - -), 0.2 (· · · ·), 0.3 (— · —), 0.4 (— · · —), 0.5 (. . . .), and 0.6 (——).

data. The lowered ideal additivity curve for 14:0–16:0 PC-sterol mixtures (at 30 mN/m) gives a misleading impression regarding a large positive deviation from ideality for experimental values at high sterol mole fraction.

### Androsterol and 6-ketocholestanol are less effective than cholesterol at reducing the lateral elasticity of SMs and their chain-matched PCs

In a previous analysis of cholesterol's effect on chain-matched SMs and PCs (Li et al., 2001), we found that cholesterol mole fractions >0.2–0.3 markedly decreased the lateral elasticity of both SMs and PCs, but that higher $C_s^{-1}$ values occurred in the SMs compared to the PCs. The data obtained here indicate that cholesterol is much more effective than either androsterol or 6-ketocholesterol at decreasing the lateral elasticity of SM and PC. At equivalent sterol mole fractions of ≥0.3, the following hierarchy in capacity to reduce the lateral elasticity of SMs or PCs was observed: *cholesterol* > *6-ketocholestanol* ≥ *androsterol*.

### Sterol structure affects 24:0 SM and 26:0 SM lateral packing elasticity

To establish the extent to which chain length asymmetry in SM influences interaction with different sterols, the surface pressure ($\pi$) versus mean molecular area (*upper panels*) and the surface compressional moduli ($C_s^{-1}$) versus mean molecular area (*lower panels*) responses were determined for androsterol, 6-ketocholestanol, and cholesterol mixed with either 24:0 SM (Fig. 6) or 26:0 SM (Fig. 7). Even with the long saturated acyl chains, two-dimensional pressure-induced phase transitions were evident in the SM isotherms in the absence of sterol (Figs. 6 and 7; *upper panels*, *far right isotherms*). In contrast to the relatively large difference in the two-dimensional phase transition onset pressures and areas between 16:0 SM (~21 mN/m; ~57 Å$^2$/molecule) and 18:0 SM (~8 mN/m, ~65 Å$^2$/molecule), those of 24:0 SM and 26:0 SM were very similar (~6–7 mN/m; ~78 Å$^2$/molecule). The data in Figs. 6 and 7 also show that elimination of the two-dimensional phase transitions in 24:0 SM and 26:0 SM required much higher mole fractions of androsterol and 6-ketocholesterol than were needed for 16:0 SM and 18:0 SM, as indicated by the characteristic troughs in the $C_s^{-1}$ versus average molecular area plots. In this regard, androsterol and 6-ketocholesterol differed significantly from cholesterol.

Fig. 8 illustrates how increasing mole fractions of androsterol, 6-ketocholestanol, and cholesterol affected the lateral elasticity of 24:0 SM and 26:0 SM at various constant surface pressures. Noteworthy are the effects of each sterol at 30 mN/m, a surface pressure that simulates biomembrane conditions with respect to lipid cross-sectional areas. At low mole fraction of either sterol mixed with the SMs (Fig. 8, ♦),

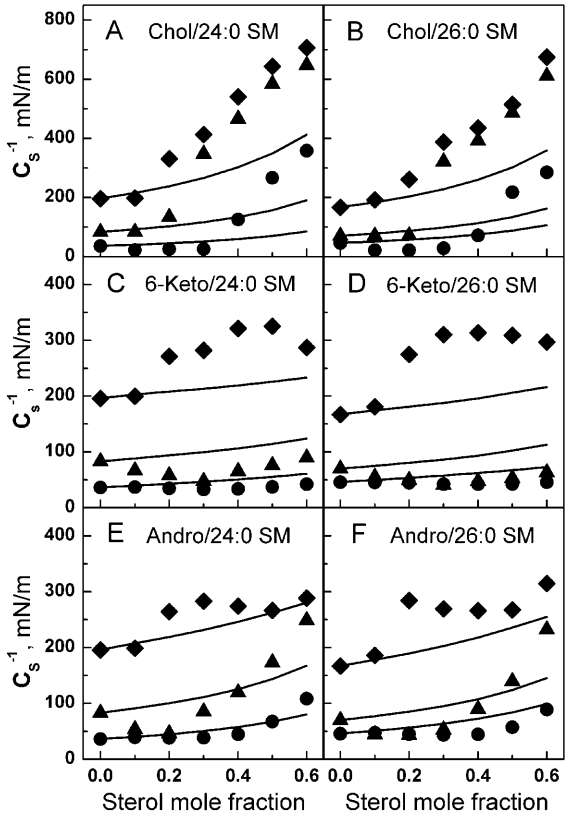


FIGURE 8 Surface compressional moduli ($C_s^{-1}$) vs. sterol mole fraction for mixed monolayers. (*A*) Cholesterol/24:0 SM; (*B*) Cholesterol/26:0 SM; (*C*) 6-ketocholestanol/24:0 SM; (*D*) 6-ketocholestanol/26:0 SM; (*E*) androsterol/24:0 SM; and (*F*) androsterol/26:0 SM. The different symbols represent values calculated from experimental data at the following surface pressures: 5 mN/m (●), 15 mN/m (▲), and 30 mN/m (♦). Solid lines represent predicted response assuming additivity of individual lipid components (see Materials and Methods).

the decreases observed in the $C_s^{-1}$ values at low sterol content (e.g., ~10–15 mol %) in 16:0 SM and 18:0 SM were not evident in the 24:0 SM and 26:0 SM. Rather, adding 10 mol % sterol produced little change in the $C_s^{-1}$ values of 24:0 SM and 26:0 SM. Increasing sterol content >10 mol % resulted in elevated $C_s^{-1}$ values, depending on sterol structure and mole fraction.

In Fig. 8, the solid lines represent theoretical ideal mixing calculated from the $C_s^{-1}$ values of pure sterol and pure 24:0 SM (or 26:0 SM) and apportioned according to both mole fraction and area fraction. At low surface pressures (e.g., 5 mN/m, ●), the lateral elasticity is relatively unaffected, but are slightly below the theoretical ideal mixing between 0 and 0.6 mole fraction of androsterol or 6-ketocholestanol in both 24:0 SM and 26:0 SM (Fig. 8, *lower solid lines*). In contrast, with cholesterol, when mole fraction exceeds 0.3–0.35, significant positive deviations occur in the $C_s^{-1}$ values compared to theoretical ideal mixing (Fig. 8, *A* and *B*). At high surface pressures (e.g., 30 mN/m), the already high $C_s^{-1}$ values characteristic of the condensed phase SM increased dramatically above sterol mole fraction of 0.1 and showed strong positive deviations from theoretical ideal mixing. The deviations from theoretical ideal mixing were strongest for cholesterol, moderate for 6-ketocholestanol, and weakest for androsterol. With cholesterol, the strong positive deviations persisted and increased with increasing sterol content in the range of 0.1–0.6 mole fraction. With 6-ketocholestanol, the more moderate positive deviations increased up to sterol mole fractions of 0.3–0.4, but further increases in sterol content did not elevate $C_s^{-1}$ values any further. With androsterol, only slight increases in $C_s^{-1}$ values were observed up to 0.3 mole fraction sterol, followed by decreasing $C_s^{-1}$ values at higher sterol mole fraction. Thus, overall, cholesterol was much more effective than either androsterol or 6-ketocholesterol at decreasing the lateral elasticity of 24:0 SM and 26:0 SM. At equivalent sterol mole fraction of 0.3 or higher, the following hierarchy was observed with respect to capacity to reduce the lateral elasticity of long chain SMs: *cholesterol > 6-ketocholestanol > androsterol*.

## Detergent resistance of SM-sterol and PC-sterol mixtures

Low lateral elasticity in cholesterol-SM bilayers has been identified as an important physical feature of LO phase that correlates with detergent resistance, a characteristic property of sphingolipid-sterol rafts (Li et al., 2001). To evaluate whether a similar correlation exists for 6-ketocholestanol-SM and androsterol-SM mixtures, their $C_s^{-1}$ values were compared with their detergent resistance. Fig. 9 (*lower panels*) shows the percent change in optical density observed after incubation with Triton X-100 for 12 h. For comparison, data also are included showing how cholesterol affects the detergent resistance of SM and PC.

When mixed with androsterol, 14:0–16:0 PC and 14:0–18:0 PC (Fig. 9 *B*, ○ and ▽) were completely solubilized by Triton X-100 at all mole fractions of sterol, in agreement with previous reports indicating a lack of detergent resistance by androsterol/DPPC mixtures (Xu and London, 2000; Xu et al., 2001). In contrast, resistance to solubilization by Triton X-100 increased moderately with 16:0 SM and 18:0 SM at androsterol mole fraction of 0.3 or higher (Fig. 9 *B*, ● and ▼). The insolubility levels (30–50%) were similar to those observed with pure 24:0 SM (Fig. 9 *B*, (♦). Increasing androsterol content in 24:0 SM actually decreased resistance to solubilization by Triton X-100 ~2–3-fold. Close inspection of the data for the various SM and PC species revealed two groupings of the $C_s^{-1}$ values at higher androsterol content (Fig. 9 *A*; 0.4 and 0.5 mole fraction). 16:0 SM (●) and 18:0 SM (▼) achieved $C_s^{-1}$ values approaching 400 mN/m and showed moderately increased resistance to solubilization by Triton X-100. In contrast, 14:0–16:0 PC (○), 14:0–18:0 PC (▽), and 24:0 SM (♦) attained lower $C_s^{-1}$ values (250–300 mN/m) and showed virtually no resistance to solubilization by Triton X-100.

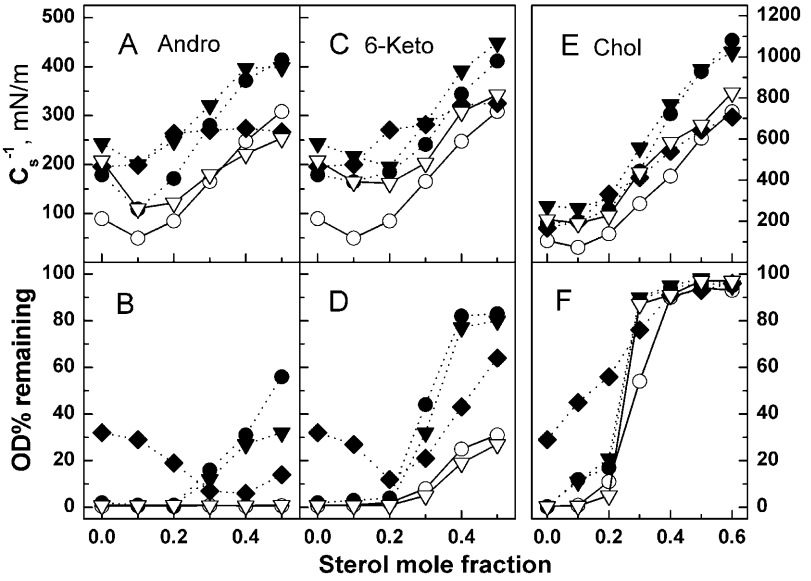


FIGURE 9 Comparison of monolayer surface compressional moduli ($C_s^{-1}$) and bilayer detergent insolubility of lipid mixtures composed of different sterols and SM or PC species. (*Upper panels*) Surface compressional modulus ($C_s^{-1}$) vs. sterol mole fraction at 30 mN/m and 24°C. (*Lower panels*) Percent optical density remaining vs. sterol mole fraction at 24°C. Symbols correspond to: 16:0 SM, (●), 14:0–16:0 PC (○),18:0 SM (▼), 14:0–18:0 PC (▽), and 24:0 SM (♦), mixed with the indicated amount of androsterol (*A* and *B*), 6-ketocholestanol (*C* and *D*), or cholesterol (*E* and *F*). The data for 24:0 SM in *E* and *F* were not part of the figure published previously (Li et al., 2001).

With 6-ketocholestanol mixtures (Fig. 9, *C* and *D*), resistance to Triton X-100 solubilization increased from nearly zero to ~65–80% for all the SMs over the sterol mole fractions range of 0.2–0.4 (Fig. 9 *D*, *solid symbols*). In contrast, detergent resistance for mixtures of 14:0–16:0 PC or of 14:0–18:0 PC and 6-ketocholestanol increased much more moderately (0–25%) over the same sterol mole fraction range (Fig. 9 *D*, *unfilled symbols*). Also, close inspection of the data for the various SM and PC species revealed two groupings of the $C_s^{-1}$ values at higher 6-ketocholestanol content (Fig. 9 *C*; 0.4 and 0.5 mole fraction). 16:0 SM (●) and 18:0 SM (▼) attained $C_s^{-1}$ values of 400–425 mN/m and showed dramatic increases in Triton X-100 resistance. In contrast, 14:0–16:0 PC (○) and 14:0–18:0 PC (▽) reached $C_s^{-1}$ values of only ~300 mN/m and showed moderate increases in resistance to solubilization by Triton X-100 (25–30%). The exception to the pattern was 24:0 SM (♦) and 6-ketocholestanol mixtures, in which there was no evidence of an apparent correlation between Triton X-100 resistance and $C_s^{-1}$ value. In this case, ~65% detergent resistance was still observed even though the $C_s^{-1}$ value of equimolar 24:0 SM-6-ketocholestanol was ~325 mN/m. The differing response of the asymmetric chain length SM was not confined to 6-ketocholestanol but was also evident when cholesterol was mixed with 24:0 SM (Fig. 9, *E* and *F*, ♦). Rather than displaying a sharp rise in detergent resistance between 0.2 and 0.3 cholesterol mole fraction, as was the case with symmetric chain length SMs and PCs, a gradual increase in detergent resistance was observed for 24:0 SM over the 0–0.4 mole fraction range of cholesterol (Fig. 9 *F*, ♦).

## DISCUSSION

The present study targeted three structural features of sterols and sphingomyelin and assessed their effect on lateral elasticity in monolayers and resistance to solubilization by Triton X-100 in bilayers, a widely used method of isolating rafts from cell membranes (London and Brown, 2000; Sot et al., 2002; Luria et al., 2002). Sterol structural alterations were directed either to the polar headgroup region or to the elimination of the isooctyl hydrocarbon tail relative to cholesterol, whereas a third structural alteration involved synthetically altering the chain-length asymmetry of SM (Fig. 1). Previously, we reported an apparent correlation between lateral elasticity and resistance to solubilization by Triton X-100 in cholesterol-SM mixtures and cholesterol-disaturated PC mixtures (Li et al., 2001). This finding suggested lateral elasticity—i.e., the ease/resistance to lateral compression might be a key physical feature of the so-called LO phase that influences detergent resistance. It is worth recalling that LO and liquid-disordered phase behavior and associated physical features were originally described in modeling studies of cholesterol and DPPC mixtures in monolayers (Ipsen et al., 1987). Thus, monolayer data obtained at surface pressures relevant to biomembranes provide useful insights into features of membrane packing, especially in bilayers where changes in lipid composition significantly alter mesomorphic structure in ways that complicate the understanding of lipid-to-lipid interactions. Other molecular descriptions, i.e., regular packing distributions of cholesterol and condensed complexes, also have been advanced for describing the mixing of cholesterol and phospholipid (for reviews, see Chong and Sugár, 2002; McConnell and Radhakrishnan, 2003). In our data, the incremental increases in sterol mole fraction (5-mol % increments) are too large to provide definitive insights into which of the preceding models may be most appropriate. Thus, we employ the more widely used term, LO, to refer

to cholesterol-rich mixtures ($X_{chol}$ = 0.3–0.6). We have provided data over a wide range of surface pressures because of increasing interest among computational biophysicists who investigate lipid-to-lipid interactions and lateral organization using molecular dynamics and Monte Carlo simulation approaches. Among cell biologists, sphingolipid-cholesterol rafts have been of great interest for the past half-decade, and the following discussion emphasizes the high pressure monolayer data which are more directly comparable to the bilayer situation.

As with cholesterol (Li et al., 2001), increasing mole fraction of either 6-ketocholestanol or androsterol in SM reduces the lateral elasticity in a nonlinear fashion over the sterol mole fraction range of 0 to 0.6. The drop in the $C_s^{-1}$ values at low sterol mole fraction and at high surface pressure indicates a significant disordering effect of the sterol on the chain-ordered SM. However, as sterol mole fraction exceeds ~0.25, $C_s^{-1}$ values increase markedly, consistent with the ordering known to occur in LO phase. The effect on $C_s^{-1}$ values is similar in nature, but reduced in magnitude, to that previously reported for 16:0- or 18:0-SM mixed with cholesterol (Li et al., 2001, and references therein). Also noteworthy is the finding that, like cholesterol, 6-ketocholestanol or androsterol at mole fraction >0.3 in 16:0-SM and 18:0 SM produce substantial positive deviations in $C_s^{-1}$ values from their predicted ideal additive response (Figs. 4 and 5). Also, the $C_s^{-1}$ values observed at 0.5 mole fraction are 1.5- to twofold higher than values for pure condensed-phase SMs or their chain-matched PCs. The difference cannot be attributed simply to the increasing content of the less compressible sterol, as indicated by additivity plots. Rather, the differing features of the LO and condensed (gel) phase states themselves are likely to be responsible. In LO phase, lipid lateral diffusion rates decrease but remain significantly faster than those of gel phase lipids (Ipsen et al., 1987; Vist and Davis, 1990; Sankaram and Thompson, 1990). The higher lateral mobility of LO phase lipid can be expected to facilitate relatively rapid achievement of equilibrium packing states characterized by very low lateral elasticity compared to pure condensed (gel) phase SM or PC, in which packing defects, that increase lateral elasticity, may persist for extended time periods (Li et al., 2000, 2001). A third similarity shared by 6-ketocholestanol, androsterol, and cholesterol is their capacity to lower the lateral elasticity of 16:0 or 18:0 SM to a greater extent than their chain-matched PCs. Although the trend is similar, the magnitude of the cholesterol effect is much greater than that of either the 6-ketocholestanol or androsterol. To better appreciate the reasons for the diminished effects of 6-ketocholestanol or androsterol, it is helpful to consider the structural similarities and differences of these sterols relative to cholesterol.

6-ketocholestanol is structurally similar to cholesterol, except that a keto group at carbon 6 replaces the 5,6 double bond in the sterol ring (Fig. 1). The rather low $C_s^{-1}$ values of 109, 169, and 233 mN/m at 10, 20, and 30 mN/m measured for pure 6-ketocholestanol monolayers (compared to $C_s^{-1}$ values of 1126, 1551, and 1540 mN/m at 10, 20, and 30 mN/m, respectively, for pure cholesterol monolayers) suggest that the presence of the 3-OH and 6-keto group in close proximity disturbs the planar nature of the sterol ring structure. Having these polar moieties positioned near the hydrocarbon-water interface of SM (or PC) causes reorientation of the 6-ketocholestanol molecule in the bilayer compared to cholesterol, consistent with the keto group being hydrated and not buried in the bilayer hydrocarbon matrix (Simon et al., 1992). Molecular dynamics simulations indicate that the positioning of 6-ketocholestanol provides for increased hydrogen bonding between water and the 6-keto group (Smondyrev and Berkowitz, 2001). The net effect is for the molecule to be tilted relative to the bilayer plane and extend ~6 Å less into the membrane than cholesterol does. A consequence of the 6-ketocholestanol positioning in the bilayer is an increased average molecular area and a diminished capacity to alter the lateral elasticity of SM and PC compared to cholesterol. In addition to having a larger and more hydrated headgroup region, the shallower penetration of 6-ketocholestanol into the hydrocarbon chains of the SMs and PCs can be expected to impart larger *free volumes* (additional gauche conformers and more disorder) to the chains resulting in diminished van der Waals attractive interactions. The net result of the altered polar headgroup region is a strong reduction in the capacity of 6-ketocholestanol to interact with SM (or PC) in ways that diminish lateral elasticity.

Androsterol lacks the isooctyl chain of cholesterol. The destabilizing effect resulting from the loss of the isooctyl chain is evident in the $C_s^{-1}$ values of 361, 393, and 324 mN/m at 10, 20, and 30 mN/m, respectively, for pure androsterol monolayers. Also, compared to mixtures of cholesterol and SM (or PC), the missing isooctyl chain enhances lateral elasticity in mixtures of androsterol and SM (or PC) presumably because of reduced van der Waals attractive interactions with the adjacent SM or PC hydrocarbon chains. To minimize the void created by the missing isooctyl chain in androsterol, the number of *gauche* rotomers increases in the region near the methyl groups of sphingomyelin's hydrocarbon chains (Davies et al., 1990) because of the increased hydrophobic mismatch. The preceding scenario appears plausible for several reasons. Previous studies have revealed that the fused tetracyclic sterol ring is hydrophobic, stereochemically rigid, ~9 Å in length, and restricts the conformational disorder of adjacent acyl chains in PC to a depth of ~11 Å from the interfacial region (Hubbell and McConnell, 1971; Rothman and Engelman, 1972; Huang, 1977; Davies et al., 1990). Because one methylene unit increases the length of the hydrocarbon chain by ~1.19–1.24 Å (Seddon et al., 1984), hydrocarbon chains will be ordered to a depth equivalent to ~9 methylene units by adjacent planar sterol rings. Thus,

16:0 SM, 18:0 SM, 14:0–16:0 PC, and 14:0–18:0 PC can all be expected to show considerable hydrophobic mismatch with respect to androsterol, but not with cholesterol. Previous studies involving homogeneous disaturated PCs suggest that minimizing hydrophobic mismatch is important for maximizing interaction with sterols. PCs with 17-carbon acyl chains interact maximally with cholesterol compared to PCs with shorter or longer acyl chains (Wu and Chi, 1991; McMullen et al., 1993) and PCs with myristoyl acyl chains interact maximally with androsterol (Ohvo-Rekilä et al., 1998). Thus, it is clear that the nonpolar isooctyl chain of cholesterol plays a significant role in reducing lateral elasticity when mixed with SM (or PC).

## SM acyl chain length effects

Changing sterol structure is not the only way that lateral elasticity can be modulated by raft lipids. Lengthening the acyl chain of SM so as to produce *intramolecular* hydrophobic mismatch, i.e., chain-length asymmetry, also dramatically affects the $C_s^{-1}$ values. SM species with very long saturated acyl chains are biologically important in both nonpathogenic and pathogenic situations. 24:0 SM is the predominant SM species in human and cow milk, in rat lung, and in *Pneumocystis carinii*, an opportunistic protist that causes pneumonia (Bitman et al., 1984; Karlsson et al., 1998; Guo et al., 1996). 24:0 and 26:0 SM become highly elevated in the tissues of humans afflicted with adrenoleukodystrophy (Wilson and Sargent, 1993). Upon mixing 24:0 SM or 26:0 SM with cholesterol, 6-ketocholestanol, or androsterol, little change is observed at 0.1 mole fraction sterol compared to the pure SM (Fig. 8). At >0.1 mole fraction sterol, the $C_s^{-1}$ values increase and deviate from predicted additivity, but much more dramatically with cholesterol than with either 6-ketocholestanol or androsterol. The steady increases in $C_s^{-1}$ values observed as a function of increasing cholesterol mole fraction in 24:0 or 26:0 SM are not observed with the other two sterols. Rather, only moderate increases in $C_s^{-1}$ values are observed between 0.1 and 0.3 mole fraction for 6-ketocholesterol or androsterol with no further increase in $C_s^{-1}$ at higher sterol mole fraction. The behavior suggests more limited miscibility of the 6-ketocholestanol and androsterol compared to cholesterol. Also noteworthy are the lower $C_s^{-1}$ values (30–35%) observed when high levels of cholesterol (>0.3 mole fraction) are mixed with 24:0 or 26:0 SM compared to 16:0 or 18:0 SM (Li et al., 2001). Nonetheless, the $C_s^{-1}$ values observed for equimolar cholesterol and 24:0 or 26:0 SM are similar in magnitude to those observed for equimolar cholesterol-DPPC (Li et al., 2001). Thus, despite the hydrophobic mismatch that can be expected when 24:0 or 26:0 SM interacts with cholesterol, relatively low lateral elasticity still occurs and enables strong resistance to solubilization by Triton X-100. Our results are consistent with previous findings showing subtle differences in the thermotropic mixing behavior of cholesterol with 16:0 SM versus 24:0 SM (Estep et al., 1979) and suggest that the acyl chain length of SM does affect the ideality of its mixing with cholesterol, in agreement with earlier modeling studies (Snyder and Freire, 1980). Although it is tempting to attribute the changes in $C_s^{-1}$ values observed with the asymmetric chain-length SMs to the monolayer organizational assembly in which stabilizing contributions caused by transbilayer interdigitation are prevented, this may not entirely be the case, inasmuch as high cholesterol content prevents transbilayer interdigitation (McIntosh et al., 1992; Maulik and Shipley, 1996).

## Is there a link between low lateral elasticity and resistance to solubilization by Triton X-100?

In our previous study of cholesterol mixing with symmetric chain SMs and their chain-matched PC derivatives (Li et al., 2001), cholesterol mole fractions sufficient to induce liquid-ordered phase behavior were shown to dramatically reduce the lateral elasticity of SMs and PCs at biologically relevant surface pressures. When $C_s^{-1}$ values were ~500 mN/m or greater, nearly complete resistance to solubilization by Triton X-100 (~90%) was observed regardless of whether the host lipid was SM or PC. The results of the present study show that structural changes to sterol or to SM can substantially affect their lateral elasticity and solubilization by Triton X-100. For instance, compared to cholesterol, androsterol only moderately lowers the lateral elasticity of SMs and saturated chain PCs, with $C_s^{-1}$ values reaching ~400–425 and ~250–325 mN/m, respectively, at equimolar sterol. Not surprisingly, androsterol shows no capacity to enhance the detergent resistance of 14:0–16:0 PC or 14:0–18:0 PC and only marginal capacity to enhance the detergent resistance of SM. However, the situation is more complex in mixtures of 6-ketocholestanol and 16:0 or 18:0 SM as well as in mixtures of long-chain SMs with either sterol. Even though 40 mol % 6-ketocholestanol and 50 mol % androsterol in 16:0 or 18:0 SM produce similar $C_s^{-1}$ values between 350 and 400 mN/m, the 6-ketocholestanol-SM mixtures much more strongly resist solubilization by detergent. The results described for 24:0 SM mixed with either 6-ketocholestanol or with androsterol also show complex patterns that do not support a simple ''cause and effect'' relationship, in which sterol/SM mixtures attain a threshold $C_s^{-1}$ value to display resistance to solubilization by Triton X-100. The preceding observations emphasize that the relationship between macroscopic properties such as lipid lateral elasticity and detergent solubility need not be simple. Rather, chemical potential is expected to be a key parameter in which the change in energetics associated with microscopic properties such as lipid-sterol interaction and detergent interaction with these molecules play key roles.

## IMPLICATIONS

Given the similar nature of the effect of increasing cholesterol content on the lateral elasticity in PC monolayers and bilayers (Smaby et al., 1997) and the very limited information available for sphingomyelin bilayers (McIntosh et al., 1992), the results reported here provide information of fundamental value to bilayer experimentalists, to theoretical computationalists employing molecular dynamics and Monte Carlo simulations to study lipid-lipid and lipid-protein interactions, and to membrane cell biologists. The focus here on sterol and SM structure and the resulting changes in the elastic material properties of model membranes is highly relevant for evaluating bilayer-based sorting of membrane proteins, a concept of widespread interest in the sorting of proteins within the Golgi apparatus (Bretscher and Munro, 1993) and encompassing the putative functionality of rafts (Simons and Ikonen, 1997). Indeed, a recent energetic analysis of cholesterol-induced protein sorting in SOPC-cholesterol bilayers by Lundbæk et al. (2003) points to the resistance to lateral compression/extension in bilayers as being a key material property that strongly potentiates the effects of membrane thickness changes for driving protein sorting. As pointed out previously (Smaby et al., 1996a,b, 1997), technical challenges associated with assessing the area compressibility moduli of sphingolipid bilayer vesicles by micropipette aspiration renders monolayer measurements particularly valuable for providing insights into how sphingomyelin and cholesterol structural features affect the lateral compression in model membranes. Our results support the idea that cholesterol is ideally structured for maximally reducing the lateral elasticity of membrane sphingolipids, enabling detergent resistance, and interacting with sphingomyelins containing saturated acyl chains similar in length to their sphingoid base. Changes in the chain length of the saturated chain in SMs that produce marked hydrocarbon chain length asymmetry may provide a basis for additional dynamic heterogeneity within microdomains of biological membranes.

We gratefully acknowledge support provided by the United States Public Health Service grants HL49180 (to H.L.B.) and GM45928 (to R.E.B.), and by the Hormel Foundation.

## REFERENCES

Ahmed, S. N., D. A. Brown, and E. London. 1997. On the origin of sphingolipid/cholesterol-rich detergent-insoluble cell membranes: physiologic concentrations of cholesterol and sphingolipids induce formation of a detergent-insoluble, liquid-ordered lipid phase in model membranes. *Biochemistry.* 36:10944–10953.

Ali, S., J. M. Smaby, H. L. Brockman, and R. E. Brown. 1994. Cholesterol's interfacial interactions with galactosylceramides. *Biochemistry.* 33:2900–2906.

Ali, S., J. M. Smaby, M. M. Momsen, H. L. Brockman, and R. E. Brown. 1998. Acyl chain-length asymmetry alters the interfacial elastic interactions of phosphatidylcholine. *Biophys. J.* 74:338–348.

Bartlett, G. R. 1959. Phosphorus assay in column chromatography. *J. Biol. Chem.* 234:466–468.

Behroozi, F. 1996. Theory of elasticity in two dimensions and its application to Langmuir-Blodgett films. *Langmuir.* 12:2289–2291.

Bitman, J., L. Wood, N. R. Mehta, P. Hamosh, and M. Hamosh. 1984. Comparison of the phospholipid composition of breast milk from mothers of term and preterm infants during lactation. *Am. J. Clin. Nutr.* 40:1103–1119.

Bretscher, M. S., and S. Munro. 1993. Cholesterol and the Golgi apparatus. *Science.* 261:1280–1281.

Brown, D. A., and J. K. Rose. 1992. Sorting of GPI-anchored proteins to glycolipid-enriched membrane subdomains during transport to the apical cell surface. *Cell.* 68:533–544.

Brown, D. A., and E. London. 2000. Structure and function of sphingolipid- and cholesterol-rich membrane rafts. *J. Biol. Chem.* 275:17221–17224.

Brown, R. E. 1998. Sphingolipid organization in biomembranes: what physical studies of model membranes reveal. *J. Cell Sci.* 111:1–9.

Chávez, E., R. Moreno-Sánchez, C. Zazueta, A. Cuéllar, J. Ramirez, H. Reyes-Vivas, C. Bravo, and S. Rodriguez-Enriguez. 1996. On the mechanism by which 6-ketocholestanol protects mitochondria against uncoupling-induced $Ca^{2+}$ efflux. *FEBS Lett.* 379:305–308.

Chong, P. L.-G., and I. P. Sugár. 2002. Fluorescence studies of lipid regular distribution in membranes. *Chem. Phys. Lipids.* 116:153–175.

Cladera, J., and P. Oshea. 1998. Intramembrane molecular dipoles affect the membrane insertion and folding of a model amphiphilic peptide. *Biophys. J.* 74:2434–2442.

Davies, J. T., and E. K. Rideal. 1963. Interfacial Phenomena, 2nd. Ed. Academic Press, New York. 265.

Davies, M. A., H. F. Schuster, J. W. Brauner, and R. Mendelsohn. 1990. Effects of cholesterol on conformational disorder in dipalmitoylphosphatidylcholine bilayers. A quantitative IR study of the depth dependence. *Biochemistry.* 29:4368–4373.

Edidin, M. 2003. The state of lipid rafts: From model membranes to cells. *Annu. Rev. Biophys. Biomol. Struct.* 32:257–283.

Estep, T. N., D. B. Mountcastle, Y. Barenholz, R. L. Biltonen, and T. E. Thompson. 1979. Thermal behavior of synthetic sphingomyelin-cholesterol dispersions. *Biochemistry.* 10:2112–2117.

Evans, E., and D. Needham. 1987. Physical properties of surfactant bilayer membranes: thermal transitions, elasticity, rigidity, cohesion, and colloidal interactions. *J. Phys. Chem.* 91:4219–4228.

Franklin, J. C., and D. S. Cafiso. 1993. Internal electrostatic potentials in bilayers—measuring and controlling dipole potentials in lipid vesicles. *Biophys. J.* 65:289–299.

Guo, Z., D. H. Beach, and E. S. Kaneshiro. 1996. Fatty acid composition of the major phospholipids of *Pneumocystis carinii*: comparison with those in the lungs of normal and methylprednisolone-immunosuppressed rats. *Infect. Immun.* 64:1407–1412.

Huang, C. 1977. A structural model for the cholesterol-phosphatidylcholine complexes in bilayer membranes. *Lipids.* 12:348–356.

Hubbell, W. L., and H. M. McConnell. 1971. Molecular motion in spin-labeled phospholipids and membranes. *J. Am. Chem. Soc.* 93:314–326.

Ipsen, J. H., G. Karlstrom, O. G. Mouritsen, H. Wennerstrom, and M. H. Zuckermann. 1987. Phase equilibria in the phosphatidylcholine-cholesterol system. *Biochim. Biophys. Acta.* 905:162–172.

Kaganer, V. M., H. Möhwald, and P. Dutta. 1999. Structure and phase transitions in Langmuir monolayers. *Rev. Mod. Phys.* 71:779–819.

Karlsson, A. Å., P. Michélsen, and G. Odham. 1998. Molecular species of sphingomyelin: determination by high-performance liquid chromatography/mass spectrometry with electrospray and high-performance liquid chromatography/tandem mass spectrometry with atmospheric pressure chemical ionization. *J. Mass Spectrom.* 33:1192–1198.

Li, X. M., J. M. Smaby, M. M. Momsen, H. L. Brockman, and R. E. Brown. 2000. Sphingomyelin interfacial behavior: The impact of changing acyl chain composition. *Biophys. J.* 78:1921–1931.

Li, X. M., M. M. Momsen, J. M. Smaby, H. L. Brockman, and R. E. Brown. 2001. Cholesterol decreases the interfacial elasticity and detergent solubility of sphingomyelins. *Biochemistry*. 40:5954–5963.

Li, X. M., M. Ramakrishnan, H. L. Brockman, R. E. Brown, and M. J. Swamy. 2002. *N*-myristoylated phosphatidylethanolamine: Interfacial behavior and interaction with cholesterol. *Langmuir*. 18:231–238.

London, E., and D. A. Brown. 2000. Insolubility of lipids in Triton X-100: physical origin and relationship to sphingolipid/cholesterol membrane domains (rafts). *Biochim. Biophys. Acta*. 1508:182–195.

Lundbæk, J. A., O. S. Andersen, T. Werge, and C. Nielsen. 2003. Cholesterol-induced protein sorting: An analysis of energetic feasibility. *Biophys. J*. 84:2080–2089.

Luria, A., V. Vegelyte-Avery, B. Stith, N. M. Tsvetkova, W. F. Wolkers, J. H. Crowe, F. Tablin, and R. Nuccitelli. 2002. Detergent-free domain isolated from Xenopus egg plasma membrane with properties similar to those of detergent-resistant membranes. *Biochemistry*. 41:13189–13197.

MacDonald, R. C. 1996. The relationship and interactions between lipid bilayer vesicles and lipid monolayers at the air/water interface. *In* Vesicles. M. Rosoff, editor. Marcel Dekker, New York, NY. 3–48.

Marsh, D. 1996. Lateral pressure in membranes. *Biochim. Biophys. Acta*. 1286:183–223.

Mattjus, P., J. G. Molotkovsky, J. M. Smaby, and R. E. Brown. 1999. A fluorescence resonance energy transfer approach for monitoring protein-mediated glycolipid transfer between vesicle membranes. *Anal. Biochem*. 268:297–304.

Maulik, P. R., and G. G. Shipley. 1996. Interactions of *N*-stearoyl-sphingomyelin with cholesterol and dipalmitoylphosphatidylcholine in bilayer membranes. *Biophys. J*. 70:2256–2265.

McConnell, H. M., and A. Radhakrishnan. 2003. Condensed complexes of cholesterol and phospholipid. *Biochim. Biophys. Acta*. 1610:159–173.

McIntosh, T. J., S. A. Simon, D. Needham, and C. Huang. 1992. Structure and cohesive properties of sphingomyelin/cholesterol bilayers. *Biochemistry*. 31:2012–2020.

McMullen, T. P. W., R. N. A. H. Lewis, and R. N. McElhaney. 1993. Differential scanning calorimetric study of the effect of cholesterol on the thermotropic phase behavior of a homologous series of linear saturated phosphatidylcholines. *Biochemistry*. 32:516–522.

Merkel, R., and E. Sackmann. 1994. Nonstationary dynamics of excimer formation in two-dimensional fluids. *J. Phys. Chem*. 98:4428–4442.

Möhwald, H. 1995. Phospholipid monolayers. *In* Handbook of Biological Physics. R. Lipowsky and E. Sackmann, Eds. vol. 1, Elsevier Science, Amsterdam. 161–211.

Momsen, W. E., J. M. Smaby, and H. L. Brockman. 1990. The suitability of nichrome for measurement of gas-liquid interfacial tension by the Wilhelmy method. *J. Colloid Interface Sci*. 135:547–552.

Needham, D. 1995. Cohesion and permeability of lipid bilayer vesicles. *In* Permeability and Stability of Lipid Bilayers. E. A. Disalvo and S. Simon, Eds. CRC Press, Boca Raton, FL. 49–76.

Needham, D., and R. S. Nunn. 1990. Elastic deformation and failure of lipid bilayer membranes containing cholesterol. *Biophys. J*. 58:997–1009.

Ohvo-Rekilä, H., P. Mattjus, and J. P. Slotte. 1998. The influence of hydrophobic mismatch on androsterol/phosphatidylcholine interactions in model membranes. *Biochim. Biophys. Acta*. 1372:331–338.

Ohvo-Rekilä, H., B. Ramstedt, P. Leppimaki, and J. P. Slotte. 2002. Cholesterol interactions with phospholipids in membranes. *Prog. Lipid Res*. 41:66–97.

Rokitskaya, T. I., Y. N. Antonenko, and E. A. Kotova. 1997. Effect of dipole potential of a bilayer lipid membrane on gramicidin channel dissociation kinetics. *Biophys. J*. 73:850–854.

Rokitskaya, T. I., E. A. Kotova, and Y. N. Antonenko. 2002. Membrane dipole potential modulates proton conductance through gramicidin channel: Movement of negative ionic defects inside the channel. *Biophys. J*. 82:865–873.

Rothman, J. E., and D. M. Engelman. 1972. Molecular mechanism for the interaction of phospholipid with cholesterol. *Nature (London). New Biol*. 237:42–44.

Sankaram, M. B., and T. E. Thompson. 1990. Interactions of cholesterol with various glycerophospholipids and sphingomyelin. *Biochemistry*. 29:10670–10675.

Schroeder, R., E. London, and D. A. Brown. 1994. Interactions between saturated acyl chains confer detergent resistance on lipids and glycosylphosphatidylinositol (GPI)-anchored proteins. *Proc. Natl. Acad. Sci. USA*. 91:12130–12134.

Schroeder, R. J., S. N. Ahmed, Y. Z. Zhu, E. London, and D. A. Brown. 1998. Cholesterol and sphingolipid enhance the Triton X-100 insolubility of glycosylphosphatidylinositol-anchored proteins by promoting the formation of detergent-insoluble ordered membrane domains. *J. Biol. Chem*. 273:1150–1157.

Seddon, J. M., G. Cevc, R. D. Kaye, and D. Marsh. 1984. X-ray diffraction study of the polymorphism of hydrated diacyl- and dialkylphosphatidylethanolamines. *Biochemistry*. 23:2634–2644.

Silvius, J. R. 2003. Roles of cholesterol in lipid raft formation: lessons from lipid model systems. *Biochim. Biophys. Acta*. 1610:174–183.

Simon, S. A., T. J. McIntosh, A. D. Magid, and D. A. Needham. 1992. Modulation of the interbilayer hydration pressure by the addition of dipoles at the hydrocarbon/water interface. *Biophys. J*. 61:786–799.

Simons, K., and E. Ikonen. 1997. Functional rafts in cell membranes. *Nature*. 387:569–572.

Simons, K., and E. Ikonen. 2000. How cells handle cholesterol. *Science*. 290:1721–1726.

Smaby, J. M., and H. L. Brockman. 1991. A simple method for estimating surfactant impurities in solvents and subphases used for monolayer studies. *Chem. Phys. Lipids*. 58:249–252.

Smaby, J. M., H. L. Brockman, and R. E. Brown. 1994. Cholesterol's interfacial interactions with sphingomyelins and phosphatidylcholines: hydrocarbon chain structure determines the magnitude of condensation. *Biochemistry*. 33:9135–9142.

Smaby, J. M., M. Momsen, V. S. Kulkarni, and R. E. Brown. 1996a. Cholesterol-induced interfacial area condensations of galactosylceramides and sphingomyelins with identical acyl chains. *Biochemistry*. 35:5696–5704.

Smaby, J. M., V. S. Kulkarni, M. Momsen, and R. E. Brown. 1996b. The interfacial elastic packing interactions of galactosylceramides, sphingomyelins and phosphatidylcholines. *Biophys. J*. 70:868–877.

Smaby, J. M., M. Momsen, H. L. Brockman, and R. E. Brown. 1997. Phosphatidylcholine acyl unsaturation modulates the decrease in interfacial elasticity induced by cholesterol. *Biophys. J*. 73:1492–1505.

Smondyrev, A. M., and M. L. Berkowitz. 2001. Effects of oxygenated sterols on phospholipid bilayer properties: a molecular dynamics simulation. *Chem. Phys. Lipids*. 112:31–39.

Sot, J., M. I. Collado, J. L. R. Arrondo, A. Alonso, and F. M. Goni. 2002. Triton X-100-resistant bilayers: effect of lipid composition and relevance to the raft phenomenon. *Langmuir*. 18:2828–2835.

Snyder, B., and E. Freire. 1980. Compositional domain structure in phosphatidylcholine-cholesterol and sphingomyelin-cholesterol bilayers. *Proc. Natl. Acad. Sci. USA*. 77:4055–4059.

Starkov, A. A., V. I. Dedukhova, and V. P. Skulachev. 1994. 6-ketocholestanol abolishes the effect of the most potent uncouplers of oxidative phosphorylation in mitochondria. *FEBS Lett*. 355:305–308.

Starkov, A. A., D. A. Bloch, B. V. Chernyak, V. I. Dedukhova, S. E. Mansurova, I. I. Serverina, R. A. Simonyan, T. V. Vygodina, and V. P. Skulachev. 1997. 6-ketocholestanol is a recoupler for mitochondria, chromatophores and cytochrome oxidase proteoliposomes. *Biochim. Biophys. Acta*. 1318:159–172.

Vist, M. R., and J. H. Davis. 1990. Phase equilibria of cholesterol/dipalmitoylphosphatidylcholine mixtures: $^{2}H$ nuclear magnetic resonance and differential scanning calorimetry. *Biochemistry*. 29:451–464.

Voglino, L., T. J. McIntosh, and S. A. Simon. 1998. Modulation of the binding of signal peptides to lipid bilayers by dipoles near the hydrocarbon-water interface. *Biochemistry*. 37:12241–12252.

Wilson, R., and J. R. Sargent. 1993. Lipid and fatty acid composition of brain tissue from adrenoleukodystrophy patients. *J. Neurochem.* 61:290–297.

Wu, W.-G., and L.-M. Chi. 1991. Conformational change of cholesterol side chain in lipid bilayers. *J. Am. Chem. Soc*. 113:4683–4685.

Xu, X., and E. London. 2000. The effect of sterol structure on membrane lipid domains reveals how cholesterol can induce lipid domain formation. *Biochemistry*. 39:843–849.

Xu, X. L., R. Bittman, G. Duportail, D. Heissler, C. Vilcheze, and E. London. 2001. Effect of the structure of natural sterols and sphingolipids on the formation of ordered sphingolipid/sterol domains (rafts). *J. Biol. Chem.* 276:33540–33546.